

Cu(2) nuclear resonance evidence for a magnetic phase in aged 60-K superconductors $R\text{Ba}_2\text{Cu}_3\text{O}_{6+x}$ ($R = \text{Tm}, \text{Y}$)

A. V. Dooglav

*Magnetic Resonance Laboratory, Kazan State University, 420008 Kazan, Russia
and Laboratoire de Physique des Solides, Université de Paris-Sud, 91405 Orsay Cedex, France*

H. Alloul

Laboratoire de Physique des Solides, Université de Paris-Sud, 91405 Orsay Cedex, France

O. N. Bakharev

*Magnetic Resonance Laboratory, Kazan State University, 420008 Kazan, Russia
and Grenoble High Magnetic Field Laboratory, Max-Planck Institut für Festkörperforschung and Centre National de la Recherche Scientifique, BP 166, 38042 Grenoble Cedex 9, France*

C. Berthier

Grenoble High Magnetic Field Laboratory, Max-Planck Institut für Festkörperforschung and Centre National de la Recherche Scientifique, BP 166, 38042 Grenoble Cedex 9, France

A. V. Egorov

*Magnetic Resonance Laboratory, Kazan State University, 420008 Kazan, Russia
and KFA Forschungszentrum Jülich, IFF, D-52425 Jülich, Germany*

M. Horvatic

Grenoble High Magnetic Field Laboratory, Max-Planck Institut für Festkörperforschung and Centre National de la Recherche Scientifique, BP 166, 38042 Grenoble Cedex 9, France

E. V. Krjukov

Magnetic Resonance Laboratory, Kazan State University, 420008 Kazan, Russia

P. Mendels

Laboratoire de Physique des Solides, Université de Paris-Sud, 91405 Orsay Cedex, France

Yu. A. Sakhratov and M. A. Teplov

Magnetic Resonance Laboratory, Kazan State University, 420008 Kazan, Russia

(Received 17 November 1997)

It is widely believed that the long-range antiferromagnetic order in the $R\text{Ba}_2\text{Cu}_3\text{O}_{6+x}$ compounds ($R = \text{Y}$ and rare earths except for Ce, Pr, Tb) is totally suppressed for the oxygen index $x \geq 0.4$ (antiferromagnetic insulator-metal transition). We present the results of the copper nuclear quadrupole resonance/NMR studies of aged $R\text{Ba}_2\text{Cu}_3\text{O}_{6+x}$ ($R = \text{Tm}, \text{Y}$) samples showing that a magnetic order can still be present at oxygen contents x up to at least 0.7 and at temperatures as high as 77 K. [S0163-1829(98)08717-7]

I. INTRODUCTION

An enormous number of papers, both experimental and theoretical, is devoted to the NMR and nuclear quadrupole resonance (NQR) studies of copper in superconducting $\text{YBa}_2\text{Cu}_3\text{O}_{6+x}$ layered cuprates. It is well known that in non-superconducting materials ($x < 0.4$) nuclei of copper located in the CuO_2 planes experience the influence of a strong internal magnetic field $H_{\text{int}} \approx 80$ kOe, which is perpendicular to the c axis, and that in superconductors ($x > 0.4$) such field is absent and $^{63,65}\text{Cu}(2)$ nuclei with the spin $I = \frac{3}{2}$ give typical NQR spectra at frequencies of $\nu_Q \approx 25-32$ MHz, i.e., in the same frequency range as that for NQR spectra of two-fold coordinated “chain” copper $^{63,65}\text{Cu}(1)$.¹ While studying

NMR of thulium in oxygen-deficient $\text{TmBa}_2\text{Cu}_3\text{O}_{6+x}$ compounds,² we have discovered the wide and subtle absorption line (Fig. 1) that looked like the copper NMR line but could not have been attributed to the mentioned Cu(2) and Cu(1) centers with $\nu_Q \approx 25-32$ MHz and $H_{\text{int}} = 0$. We consequently undertook experiments with $\text{TmBa}_2\text{Cu}_3\text{O}_{6+x}$ samples ($x = 0.51, 0.6, 0.7$) in zero external field at $T = 4.2$ K, which allowed us to observe a Cu(2) ZFNMR spectrum completely different from those described in the literature. The results of these experiments are presented in this paper. The analysis of Cu(2) spectra of both types corresponding to $H_{\text{int}} \neq 0$ (type I, $\nu_{\text{ZFNMR}} = 55-135$ MHz) and $H_{\text{int}} = 0$ (type II, $\nu_Q \approx 25-32$ MHz) shows that each of them belongs to two varieties of Cu(2) centers, A and B, possessing different

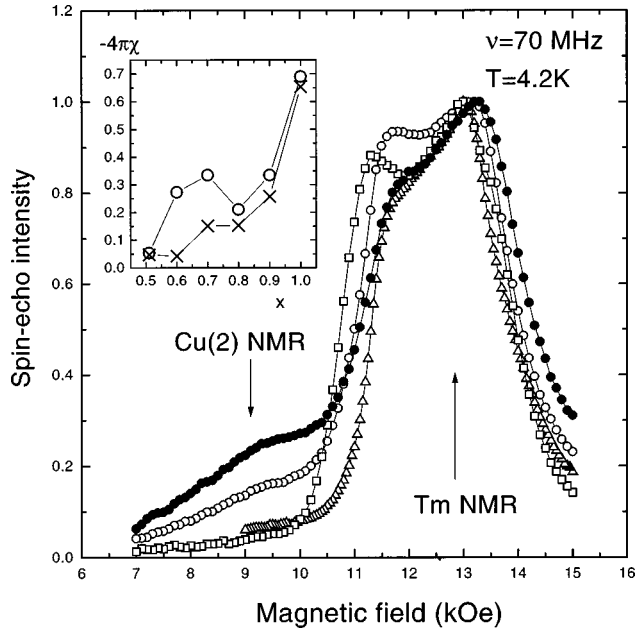


FIG. 1. Tm and Cu(2) NMR spectra of the aligned Tm6+x powders with $x=0.51$ (triangles), 0.6 (light circles), 0.7 (squares) at a frequency of 70 MHz in an external field H perpendicular to the c axis. Cu(2) NMR is particularly pronounced in the saturated spectrum of Tm6.6 (black circles) taken at a pulse sequence repetition rate of $F=100$ Hz. Inset: ac diamagnetic susceptibility of Tm6+x at liquid helium temperature (frequency of 1 kHz, $H_1 \approx 1$ Oe); circles: for 1-year-aged samples (Ref. 2), crosses: for 6-years-aged samples.

NQR frequencies and that A_I and B_I centers differ much in the value of H_{int} . Similar results are obtained for one YBa₂Cu₃O_{6.66} sample.³

II. EXPERIMENT

The TmBa₂Cu₃O_{6+x} samples used in these experiments were c -axis-oriented powders mixed with paraffin (hereafter denoted as Tm6+x). They were previously used for Tm NMR studies.² All of them were stored at room temperature for almost 6 years after preparation. Critical temperatures ($T_c^{\text{onset}}=53, 61, \text{ and } 64$ K for $x=0.51, 0.6, \text{ and } 0.7$, respectively) were obtained from measurements of the diamagnetic susceptibility at a frequency of 1 kHz. Home-built spin-echo NQR spectrometers were used for the Cu(2) NQR and ZFNMR measurements. Examples of the copper NQR spectra in Tm6.6 are shown in Fig. 2. Comparing the nonsaturated and saturated spectra [Figs. 2(a) and 2(b)] taken at 4.2 K with pulse sequence repetition rates of 1 and 200 Hz, respectively, one can distinguish two contributions with different spin-lattice relaxation times T_1 [Fig. 2(c)] and separate them [Figs. 2(d) and 2(e)] by using a simple subtraction procedure. Two narrow lines in Fig. 2(e) corresponding to the long T_1 time are believed to originate from the two-fold coordinated Cu(1)₂ sites that belong to “empty chains” surrounded by “full chains” in the CuO_x plane.¹ The broad spectrum in Fig. 2(d) characterized by the short T_1 has a two-hump shape typical for the Cu(2) NQR spectrum of an annealed sample.⁴ In the following it is denoted as the spectrum of type II. Computer simulations have shown that this

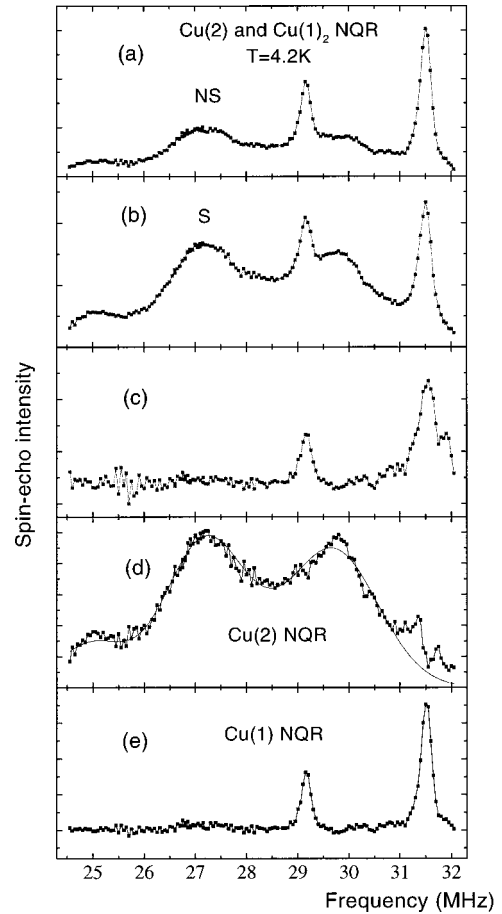


FIG. 2. Copper NQR spectra of Tm6.6 at a temperature of 4.2 K: (a) nonsaturated Cu(1) and Cu(2) spectra ($F=1$ Hz), (b) saturated Cu(1) and Cu(2) spectra ($F=200$ Hz), (c) ratio of the nonsaturated to saturated echo intensity, (d) Cu(2) NQR spectrum, (e) Cu(1) NQR spectrum. Solid line in (d) is an approximation by four Gaussians (for parameters see Table I).

two-hump spectrum can be described by a sum of four Gaussians (two sites, A_{II} and B_{II} , times two isotopes, ⁶³Cu and ⁶⁵Cu), the amounts of A_{II} and B_{II} sites appearing in a ratio of approximately $2:1$ independent of the oxygen index x . The parameters of the spectra taken with a fixed pulse separation time $\tau=25$ μ s are given in Table I for three samples studied.

The Cu(2) ZFNMR (type I) spectra taken at 4.2 K with a fixed pulse separation time $\tau=33$ μ s are shown in Fig. 3. A similar spectrum was observed in Tm6.6 at a temperature of 77 K [shown by filled squares in Fig. 3(b)]. It should be

TABLE I. Parameters of the ⁶³Cu(2) NQR spectra (type II) in Tm6+x samples at $T=4.2$ K (with no corrections for the frequency dependence and for the spin-spin relaxation time T_2).

Sample	Site	⁶³ ν_Q (MHz)	Full rms width (MHz)	Intensity
Tm6.51	A_{II}	29.44(2)	1.35(3)	0.65(1)
	B_{II}	26.76(6)	1.17(4)	0.35(4)
Tm6.6	A_{II}	29.69(2)	1.75(4)	0.69(1)
	B_{II}	27.01(6)	1.46(4)	0.31(4)
Tm6.7	A_{II}	30.36(3)	2.02(6)	0.68(1)
	B_{II}	27.39(6)	1.79(9)	0.32(2)

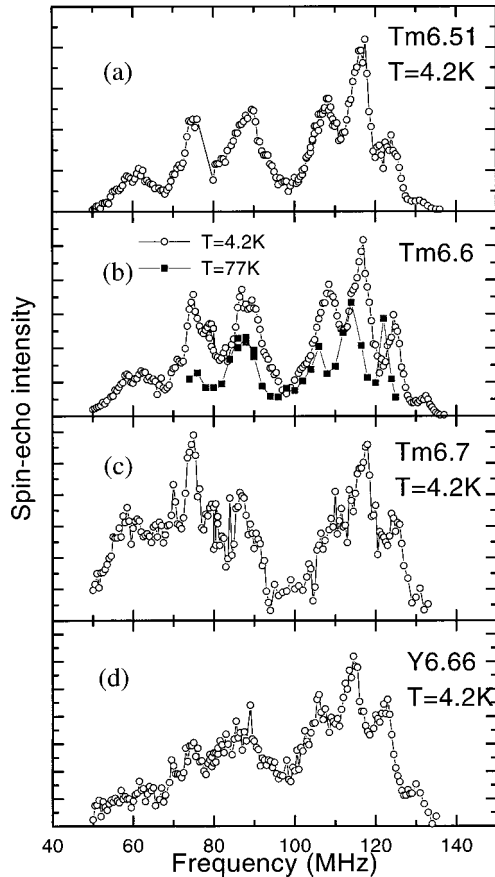


FIG. 3. Cu(2) ZFNMR spectra of (a) Tm6.51, (b) Tm6.6, (c) Tm6.7, and (d) Y6.66 at a temperature of 4.2 K. Black squares in (b) is the spectrum at $T=77$ K multiplied by a factor of 10. The $\text{YBa}_2\text{Cu}_3\text{O}_{6.66}$ sample was stored at room temperature for 3 years after preparation.

noted here that in our experiments the well pronounced spectra of type I were observed only in those Tm and Y compounds that exhibited well-pronounced two-hump spectra of type II [Fig. 2(d)]. An obvious downfall of the spectral intensity at around 98 MHz that looks particularly pronounced at $x=0.7$ clearly shows that the ZFNMR spectrum is also composed of two contributions: those are the low-frequency fragment (LFF) at 55–98 MHz and the high-frequency fragment (HFF) at 98–135 MHz.

In order to estimate the integrated intensities, S_I and S_{II} , of the ZFNMR (type I) and NQR (type II) spectra, we have corrected them according to the spin-spin relaxation times T_2 measured at the main peaks of the spectra. All spin-echo decays measured at 4.2 K have been found to obey the following formula: $A_{2\tau}/A_0 = \exp[-(2\tau/T_2)^n]$. In the series of Tm compounds, the longest T_2 times were measured for the Tm6.6 sample: $T_2=72, 64, 119, 75, 43,$ and $54 \mu\text{s}$ at frequencies of 62, 74, 87, 109, 116, and 124 MHz, respectively; the values of n were found to lie in the range 0.7–0.9. Because of the broad frequency range the echo intensity has also been corrected by a factor ν^2 , one factor ν due to the nuclear magnetization, the other one due to the precession frequency of the nuclear magnetization. The T_2 -correction procedure consisted of four steps: (i) fitting the experimental Cu(2) spectra by a superposition of Gaussians (6 for type I and 4 for type II); (ii) multiplying intensity of each compo-

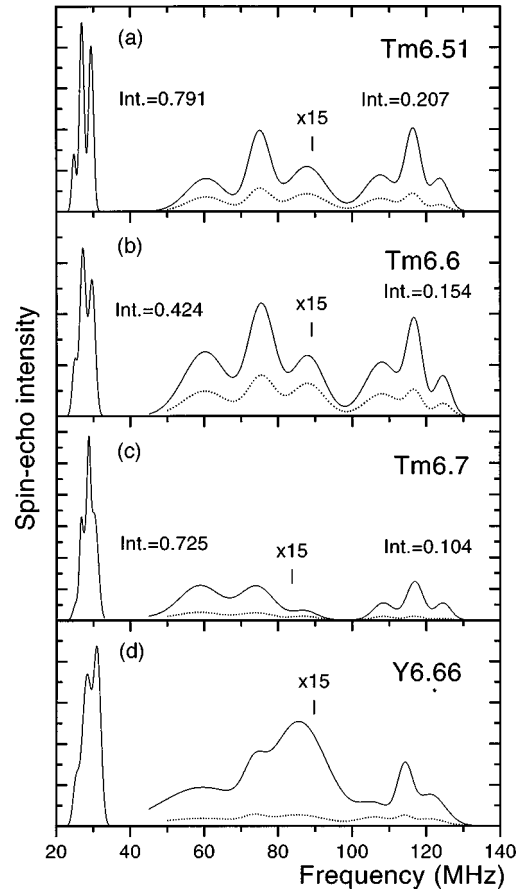


FIG. 4. Calculated Cu(2) NQR and ZFNMR spectra of (a) Tm6.51, (b) Tm6.6, (c) Tm6.7, and (d) Y6.66 obtained from the experimental spectra of Fig. 3 as a superposition of six Gaussians: solid lines $F_0(\nu)$ —taking into account the ν^2 -type dependence of the spin-echo intensities and the losses of signal intensities due to spin-spin relaxation, dotted lines $F_{2\tau}(\nu)$ —taking into account the ν^2 -dependence only (for details see text). The integrated intensities of the S_I and S_{II} spectra depicted by solid lines are normalized by the intensity of the Cu(2) ZFNMR spectrum of the 1 gram $\text{TmBa}_2\text{Cu}_3\text{O}_{6.1}$ sample at $T=4.2$ K. For convenience of comparison, the ZFNMR spin-echo intensities are multiplied by a factor of 15.

nent by the corresponding factor $\exp[(2\tau/T_2)^n]$; (iii) summation of the corrected Gaussian lines; (iv) ν^2 correction. The resulting spectra are shown by solid lines in Fig. 4. The results of the best fit for the Tm6.51 and Tm6.6 samples show the LFF and HFF intensities to be in a ratio $\approx 2:1$, which allows us to ascribe them, in analogy with the above type II spectrum, to the A_I and B_I sites, respectively. In Table II, the partial ratios S_{A_I}/S_{B_I} and $S_{A_{II}}/S_{B_{II}}$ for spectral intensities of the A and B sites are given along with the ratio S_{II}/S_I . The absolute values of the signal intensities per 1 gram of material, S_I and S_{II} , shown in the last column of Table II, are normalized to the intensity of the “ordinary” Cu(2) ZFNMR spectrum of the $\text{TmBa}_2\text{Cu}_3\text{O}_{6.1}$ antiferromagnet as observed at $T=4.2$ K in the frequency range from 61 to 123 MHz.

As can be seen from the last column of Table II, the volume fraction of the material contributing to the total Cu(2) resonance absorption varies from sample to sample being equal to 1.00, 0.58, and 0.83 in Tm6.51, Tm6.6, and Tm6.7, respectively, as compared to Tm6.1. Since the Cu(2)

TABLE II. Intensities of the Cu(2) spectra in Tm6+x ($x=0.51, 0.6, 0.7$) and Y6.66 at T=4.2 K.

Sample	ZFNMR		NQR		NQR/ZFNMR
	S_{A1}/S_{B1}		S_{AII}/S_{BII}		S_{II}/S_I
	Lorentzian approximation with the T_2 corrections	Gaussian approximation with the T_2 corrections	Gaussian approximation with no T_2 corrections	Gaussian approximation with the T_2 corrections	Gaussian approximation with the T_2 corrections
Tm6.51	1.6(3)	1.6(4)	1.8(2)	1.8(6)	0.791/0.207=3.8(1.3)
Tm6.6	2.0(2)	2.0(5)	2.2(2)	2.0(7)	0.424/0.154=2.8(9)
Tm6.7		3.7(1.2)	2.1(2)	2.5(9)	0.725/0.104=7(2)
Y6.66		3.3(1.2)	2.6(9)	3.8(1.3)	3.7(1.3)

ZFNMR spectrum is certainly produced by a nonsuperconductor, the question arises: What part of the Cu(2) NQR signal intensity can be attributed to the superconducting fraction? To answer this question, we have remeasured the ac diamagnetic susceptibility of the Tm6+x samples ($x=0.51-1.0$)² at a temperature of 4.2 K. The results of the measurements (see inset in Fig. 1) clearly show that the superconducting fraction decreases with aging time (with no changes in T_c), the tendency being most pronounced for the 60-K superconductors, and that the superconducting fraction of the 6-year-old samples under study is quite small, i.e., 0.05, 0.05, and 0.15 for Tm6.51, Tm6.6, and Tm6.7, respectively. Comparing the latter quantities with the Cu(2) NQR signal intensities (0.79, 0.42, and 0.73, respectively), one arrives at the conclusion that at least a part of the Cu(2) absorption observed at 4.2 K definitely originates from the non-superconducting material. This conclusion is also supported by the fact that in one of the samples studied, YBa₂Cu₃O_{6.66}, which was prepared quite recently, we did not observe a two-hump NQR, nor a ZFNMR spectrum.³

III. DISCUSSION

In order to clarify the origin of the LFF and HFF spectra, we have tried to fit the Cu(2) ZFNMR in a correct way assuming that the A_1 and B_1 sites can be characterized by different values of ν_Q , H_{int} , and θ (angle between \mathbf{H}_{int} and the c axis). Prior to fitting the experimental spectra (Fig. 3) have been T_2 corrected by the function $f(\nu) = F_0(\nu)/F_{2\tau}(\nu)$, where $F_{2\tau}(\nu)$ is the ZFNMR spectrum shown in Fig. 4 by a dotted line, and $F_0(\nu)$ is the spectrum represented by a solid line. The spectra of Tm6.51 and Tm6.6 corrected in this way are shown in Fig. 5. The fitting procedure included numeric diagonalization of the two Hamiltonians and calculation of all the transitions probabilities ($\sim \nu^2$). When calculating averaged values of the probabilities in oriented powdered samples, we have taken an orientation of a radiofrequency field with respect to the c axis into account ($\mathbf{H}_1 \perp c$). In all the cases considered, the Lorentzian shape of an individual resonance line was found to fit the experimental data much better than the Gaussian one. Two versions of the fit have been considered. When the angles θ were allowed to be free, the best fit of the Cu(2) ZFNMR spectrum of Tm6.51 was obtained at the following parameters [see solid line in Fig. 5(a)]:

“ θ free”,

$$A_1\text{-sites, } \nu = 55-98 \text{ MHz, intensity } S_{A1} = 62(6)\%, \quad (1)$$

$$\theta = 82(4)^\circ, H_{\text{int}} = 63.9(3) \text{ kOe, } \nu_Q = 31(2) \text{ MHz,}$$

$$B_1\text{-sites, } \nu = 98-127 \text{ MHz,}^5 \text{ intensity } S_{B1} = 38(3)\%,$$

$$\theta = 64(1)^\circ, H_{\text{int}} = 97.7(2) \text{ kOe, } \nu_Q = 25(2) \text{ MHz,} \quad (2)$$

linewidth FWHM = 4.4(4) MHz.

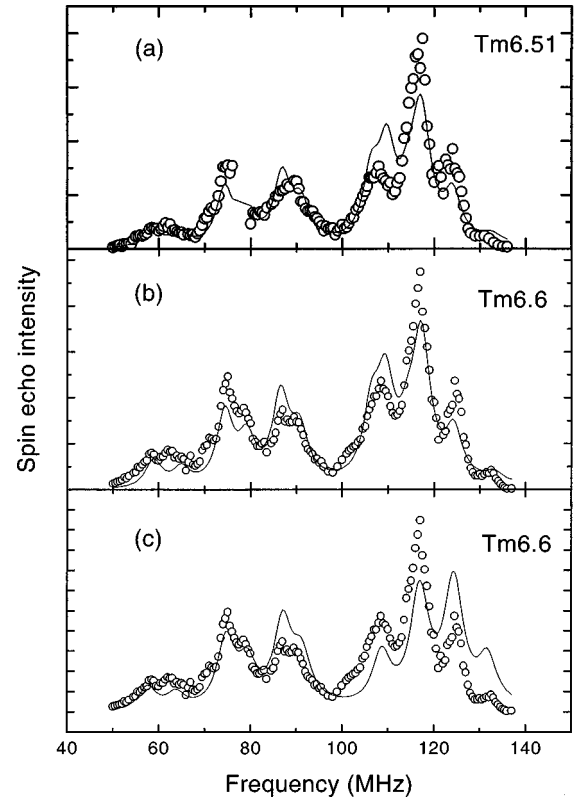


FIG. 5. Cu(2) ZFNMR spectra of (a) Tm6.51 and (b) Tm6.6 obtained from the experimental spectra of Figs. 3(a) and 3(b) by taking into account the losses of signal intensities due to spin-spin relaxation (for details see text). Solid lines in (a) and (b) represent the results of the numerical diagonalization of the two Hamiltonians with the parameters given in Eqs. (1)–(4); solid line in (c) represents the spectrum of Tm6.6 calculated with the parameters given in Eqs. (5) and (6).

The corresponding parameters for the Tm6.6 sample have been obtained as follows [Fig. 5(b)]:

$$A_{\Gamma}\text{-sites, } \nu=55\text{--}98 \text{ MHz, } S_{A_{\Gamma}}=66(4)\%, \quad (3)$$

$$\theta=83(3)^{\circ}, \quad H_{\text{int}}=64.1(2) \text{ kOe, } \nu_Q=30(1) \text{ MHz,}$$

$$B_{\Gamma}\text{-sites, } \nu=98\text{--}127 \text{ MHz,}^5 \quad S_{B_{\Gamma}}=34(2)\%,$$

$$\theta=63.5(5)^{\circ}, \quad H_{\text{int}}=97.6(1) \text{ kOe, } \nu_Q=27(1) \text{ MHz,} \quad (4)$$

$$\text{FWHM}=4.4(3) \text{ MHz.}$$

In the second version ($\theta=90^{\circ}$) both internal fields were assumed to lie in the ab plane. The results of this fit for Tm6.6 are as follows [see solid line in Fig. 5(c)]:

$$“\theta=90^{\circ}”^*,$$

$$A_{\Gamma}\text{-sites, } \nu=55\text{--}98 \text{ MHz, } \text{intensity } S_{A_{\Gamma}}=66(6)\%, \quad (5)$$

$$H_{\text{int}}=64 \text{ kOe}^*, \quad \nu_Q=30 \text{ MHz}^*,$$

$$B_{\Gamma}\text{-sites, } \nu=98\text{--}135 \text{ MHz, } S_{B_{\Gamma}}=34(3)\%,$$

$$H_{\text{int}}=103 \text{ kOe}^*, \quad \nu_Q=15.3(7) \text{ MHz,} \quad (6)$$

$$\text{FWHM}=4.8(4) \text{ MHz}$$

(* denotes the fixed parameters). The second fit seems to agree with experiment worse than the first one, but this can be due to incorrect intensities of the HFF lines deduced from the T_2 -correction procedure. We believe that at the present stage both versions can be considered satisfactory; more experimental work is needed to make a choice between them. In both cases the Cu(2) NMR line in Fig. 1 has been identified as originating from two groups of A_{Γ} lines (at 58–63 MHz and 74–79 MHz).

Then summarizing all experimental facts, one should adopt that at least a part of the two-hump NQR spectrum, which is supposed to be typical for the annealed 123 superconductors with high T_c s,⁴ and the ZFNMR spectrum, which is observed in the 60 K superconductors exhibiting a well-pronounced two-hump NQR, are actually representing a non-superconducting material. In what follows, we try to speculate about the plausible structure of this material. It is known that a structural (chemical) microphase separation takes place in the oxygen-deficient 123 superconductors.^{2,6–9} Therefore, one could naturally expect to find the defects of the crystal lattice in the form of layers (reflecting the basic property of the layered structure itself) and, following this way, could associate the two types of Cu(2) spectra with two different nonsuperconducting microphases, i.e., hole doped (type II) and nondoped (type I) layers, forming some kind of stacking sequence along the c axis.² On the other hand, the coincidence of the ν_Q values [see Eqs. (1)–(4) and Table I] in the two absolutely different phases lead us to consider that both types of Cu(2) spectra might originate from the same CuO_2 layers (bilayers).

To make a choice between these two scenarios, one should use the neutron-scattering data which gives a direct information on a magnetic structure of the oxygen-deficient

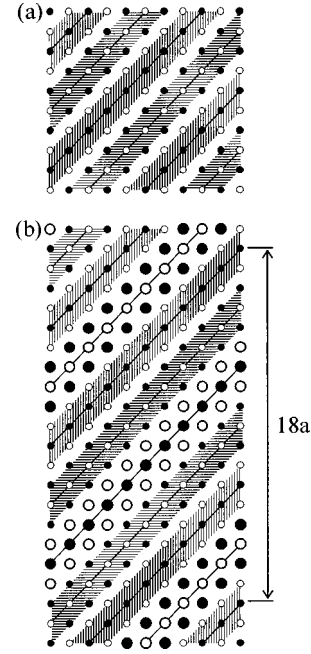


FIG. 6. Plausible stripe patterns in the (a) optimally doped [$p = \frac{1}{6}$ hole per Cu(2)] and (b) underdoped ($p = \frac{1}{9}$) CuO_2 planes. Copper atoms carrying magnetic moments of opposite orientations are shown by big light and black circles, those carrying no magnetic moments are shown by small circles, solid lines mark the centers of the nonmagnetic (hatched) and magnetic (nonhatched) stripes. The period of 18 lattice spacings of the magnetic superstructure in (b) is twice as large as the period of the charge pattern.

123 compounds. The thorough studies of the neutron scattering in $\text{YBa}_2\text{Cu}_3\text{O}_{6.6}$ (Refs. 10–13) have resulted in a recent observation¹³ of incommensurate magnetic fluctuations peaked at $\mathbf{Q} = (\frac{1}{2} \pm \delta, \frac{1}{2} \pm \delta)$ with $\delta = 0.057 \pm 0.006$ r.l.u. It was also found that the dynamical susceptibility $\chi''(\mathbf{q}, \omega)$ at the incommensurate positions first appears at temperatures somewhat above T_c and then increases on cooling below T_c , altogether with the suppression of magnetic fluctuations at the commensurate points. These observations look similar to those for the $\text{La}_{1.6-x}\text{Nd}_{0.4}\text{Sr}_x\text{CuO}_4$ compounds^{14,15} and thus can be considered as giving evidence for a formation of a static (or quasistatic) stripe pattern in the CuO_2 layers. The layer-by-layer separation scenario seems to be inconsistent with such a stripe model. On the contrary, the stripelike modulation of charge and spin densities in CuO_2 layers resulting in an inequivalency of Cu(2) sites looks very likely. Indeed, analyzing the data of Table II, one can conclude that there could exist a certain value of x_{pin} (close to 0.6) that corresponds to the following relations:

$$S_{A_{\Gamma}}/S_{B_{\Gamma}}=2, \quad S_{A_{\text{II}}}/S_{B_{\text{II}}}=2, \quad S_{\text{II}}/S_{\text{I}}=2. \quad (7)$$

These relations can be understood in the frame of the charge stripe model suggested in Ref. 16. A plausible stripe pattern corresponding to the optimally doped CuO_2 planes ($\frac{1}{6}$ hole per CuO_2 unit) is shown in Fig. 6(a). If one takes every third stripe away [Fig. 6(b)], the hole concentration p becomes $(\frac{2}{3}) \times (\frac{1}{6}) = \frac{1}{9}$. According to the empirical formula $p = 0.187 - 0.21(1-x)$, suggested by Tallon *et al.*¹⁷ for $x \geq 0.45$, the concentration $p = \frac{1}{9}$ corresponds to $x = 0.64$, which is close to

what is expected for Eq. (7) to hold. The magnetic superstructure shown in Fig. 6(b) has a period of 18 lattice spacings. This period and the diagonal direction [110] of the stripes in Fig. 6(b) exactly corresponds to the incommensurate magnetic fluctuations observed in $\text{YBa}_2\text{Cu}_3\text{O}_{6.6}$.¹³ The model in Fig. 6(b) predicts incommensurate peaks at $\mathbf{Q} = (\frac{1}{2} \pm \delta, \frac{1}{2} \pm \delta)$ with $\delta = \frac{1}{18} = 0.0556$. In this stripe pattern, it is easy to distinguish four different Cu(2) sites which could be identified as sites A_I (at borders of magnetic stripes), B_I (at centers of magnetic stripes), A_{II} (at borders of nonmagnetic stripes), B_{II} (at centers of nonmagnetic stripes). An alternative possibility is to ascribe the B_{II} sites to copper atoms located at outer borders of the nonmagnetic bi-stripes allowing the A_{II} sites to occupy four lines of coppers inside the bi-stripes. In any case, however, one has a problem to explain why the transferred hyperfine field from the A_I copper spins does not influence the NQR spectrum of the neighboring type-II copper centers. Further experimental work is necessary to better understand the allocation of the Cu(2) centers responsible for the two-hump NQR spectrum.

It is known that the observation of the static stripe-phase order of holes and spins in $\text{La}_{1.6-x}\text{Nd}_{0.4}\text{Sr}_x\text{CuO}_4$ (Refs. 14,15) has appeared possible due to pinning of the stripes by the neodymium impurities. What could be the reason for stripes to be pinned in nonstoichiometric 123 compounds? We believe that the so-called ‘‘OrthoIII’’ superstructure in CuO_x planes could cause pinning of charge stripes in CuO_2 planes since this superstructure has a period ($3a_0$) commensurate with the period of the stripe pattern shown in Fig. 6(b). A possibility for the OrthoIII to form a stable phase at $x = 0.65-0.77$ was proved by the electron,¹⁸ x-ray and neutron-diffraction¹⁹ measurements. The above oxygen contents appear to be shifted to higher values than that (x_{pin}) expected for the condition Eq. (7) to be fulfilled. However, the value of x_{pin} may happen to result from an interplay

between the OrthoIII ordering of CuO_x layers at $x > x_{\text{pin}}$ and an appropriate hole doping of CuO_2 layers ($p = \frac{1}{9}$ per CuO_2 at $x < x_{\text{pin}}$). Experiments with an $\text{YBa}_2\text{Cu}_3\text{O}_{6.77}$ single crystal¹⁹ have shown that the OrthoIII phase is stable at temperatures below 75 °C. Therefore, the interactions responsible for the formation of the OrthoIII phase seem to be rather weak and can be easily disturbed by thermally-activated oxygen diffusion. This feature of the T-x phase diagram allows us to understand why the Cu(2) ZFNMR was observed in our experiments only in those 123 superconductors that were subjected to a very long-term room-temperature annealing.

IV. CONCLUSIONS

The Cu(2) nuclear resonance spectra were studied at liquid-helium temperatures in samples of oxygen-deficient 60-K superconductors, $\text{TmBa}_2\text{Cu}_3\text{O}_{6+x}$ and $\text{YBa}_2\text{Cu}_3\text{O}_{6.66}$, stored at room temperature for a long time (up to 6 years). Cu(2) ZFNMR spectra different from those known so far were observed, indicating the presence of a nonsuperconducting phase in the superconducting samples. The quantitative analysis of the copper resonance absorption intensities in different samples lead us to consider that both types of Cu(2) spectra (ZFNMR at 55–135 MHz and at least a part of NQR at 25–32 MHz) might originate from the same nonsuperconducting CuO_2 layers decorated by the pinned charge stripes.

ACKNOWLEDGMENTS

This work was supported in part by the Russian Scientific Council on Superconductivity, under Project 94029, by the Russian Foundation for Basic Research, under Project 96-02-17058a, by the NATO Scientific and Environmental Affairs Division, under Grant No. HTEC.LG-950536, and by the INTAS, under Grant No. 96-0393.

¹I. Heinmaa, H. Lütgemeier, S. Pekker, G. Krabbes, and M. Buchgeister, *Appl. Magn. Reson.* **3**, 689 (1992).

²O. N. Bakharev, A. V. Dooglav, A. V. Egorov, O. B. Marvin, V. V. Naletov, M. A. Teplov, A. G. Volodin, and D. Wagener, in *Phase Separation in Cuprate Superconductors*, edited by E. Sigmund and K. A. Müller (Springer-Verlag, Berlin, 1994), p. 257.

³Two samples $\text{YBa}_2\text{Cu}_3\text{O}_{6.66}$ have been studied. In a sample that has been stored three years after preparation, the Cu(2) ZFNMR signal has been seen. In a most recent one (less than a year) that has been used as a reference in the YBCO:Ni work by J. Bobroff *et al.*, [*Phys. Rev. Lett.* **79**, 2117 (1997)], the Cu(2) signals A_I and B_I were not detected.

⁴A. J. Vega, W. E. Farneth, E. M. McCarron, and R. K. Bordia, *Phys. Rev. B* **39**, 2322 (1989).

⁵In the version ‘‘ θ free’’ the Cu(2) ZFNMR line at a frequency of 132 MHz (see Fig. 3) was assumed to be a forbidden transition of the A_I sites.

⁶J. Mesot, P. Allenspach, U. Staub, A. Furrer, and H. Mutka, *Phys. Rev. Lett.* **70**, 865 (1993).

⁷M. Iliev, C. Thomsen, V. Hadjiev, and M. Cardona, *Phys. Rev. B* **47**, 12 341 (1993).

⁸O. N. Bakharev, A. V. Dooglav, A. V. Egorov, E. V. Krjukov, Yu. A. Sakhratov, M. A. Teplov, H. B. Brom, and J. Witteveen, *Zh. Eksp. Teor. Fiz. Pis'ma Red.* **64**, 365 (1996) [*JETP Lett.* **64**, 398 (1996)].

⁹O. N. Bakharev, L. K. Aminov, A. V. Dooglav, A. V. Egorov, E. V. Krjukov, I. R. Mukhamedshin, V. V. Naletov, M. A. Teplov, A. G. Volodin, J. Witteveen, H. B. Brom, and H. Alloul, *Phys. Rev. B* **55**, 11 839 (1997).

¹⁰J. M. Tranquada, P. M. Gehring, G. Shirane, S. Shimoto, and M. Sato, *Phys. Rev. B* **46**, 5561 (1992).

¹¹B. J. Sternlieb, J. M. Tranquada, G. Shirane, M. Sato, and S. Shimoto, *Phys. Rev. B* **50**, 12 915 (1994).

¹²J. M. Tranquada, cond-mat/9702117 (unpublished).

¹³P. Dai, H. A. Mook, and F. Dogan, *Phys. Rev. Lett.* **80**, 1738 (1998).

¹⁴J. M. Tranquada, B. J. Sternlieb, J. D. Axe, Y. Nakamura, and S. Uchida, *Nature (London)* **375**, 561 (1995); J. M. Tranquada, J. D. Axe, N. Ichikawa, Y. Nakamura, S. Uchida, and B. Nachumi, *Phys. Rev. B* **54**, 7489 (1996).

¹⁵J. M. Tranquada, J. D. Axe, N. Ichikawa, A. R. Moodenbaugh, Y. Nakamura, and S. Uchida, *Phys. Rev. Lett.* **78**, 338 (1997).

- ¹⁶O. N. Bakharev, M. V. Eremin, and M. A. Teplov, *Zh. Eksp. Teor. Fiz. Pis'ma Red.* **61**, 499 (1995) [*JETP Lett.* **61**, 515 (1995)].
- ¹⁷J. L. Tallon, C. Bernhard, H. Shaked, R. L. Hitterman, and J. D. Jorgensen, *Phys. Rev. B* **51**, 12 911 (1995).
- ¹⁸S. Yang, H. Claus, B. W. Veal, R. Wheeler, A. P. Paulikas, and J. W. Downey, *Physica C* **193**, 243 (1992).
- ¹⁹P. Schleger, H. Casalta, R. Hadfield, N. H. Andersen, H. F. Poulsen, M. von Zimmermann, J. R. Schneider, R. Liang, P. Dosanjh, and W. N. Hardy, *Physica C* **241**, 103 (1995).